Biomaterials 29 (2008) 2776–2782

Contents lists available at ScienceDirect

Biomaterials

journal homepage: www.elsevier.com/locate/biomaterials

# Glutathione-mediated release of functional plasmid DNA from positively charged quantum dots

Dan Li [a,1], Gaiping Li [a,b,1], Weiwei Guo [a,b], Peicai Li [a,b], Erkang Wang [a,*], Jin Wang [c,**]

[a] State Key Laboratory of Electroanalytical Chemistry, Changchun Institute of Applied Chemistry, Chinese Academy of Sciences, 5625 Renmin Street, Changchun, Jilin 130022, PR China
[b] Graduate School of the Chinese Academy of Sciences, Beijing 100039, PR China
[c] Department of Chemistry, State University of New York at Stony Brook, NY 11794-3400, USA

ARTICLE INFO

*Article history:*
Received 9 January 2008
Accepted 4 March 2008
Available online 2 April 2008

*Keywords:*
QDs
Glutathione
Plasmid DNA
Controlled release

ABSTRACT

DNA was efficiently bound to water-soluble positively charged CdTe quantum dots (QDs) through complementary electrostatic interaction. These QDs–DNA complexes were disrupted and DNA was released by glutathione (GSH) at intracellular concentrations. Interestingly, there was almost no detectable DNA released by extracellular concentration of GSH. The formation of QDs–DNA complexes and GSH-mediated DNA release from the complexes were confirmed by dye displacement assay, electrophoretic mobility shift assay (EMSA), transmission electron microscopy (TEM) and X-ray photoelectron spectroscopy (XPS) experiments. The released DNA retained transcriptional activity and expressed enhanced green fluorescent protein (EGFP) after being transfected into HEK 293 cells. The transfection efficiency measured by flow cytometry (FCM) was comparable with the positive control. The obvious difference of GSH concentration in nature between the intra- and extracellular environments as well as the GSH concentration-dependent triggered release suggests potential applications of these positively QDs in selective unpacking of payload in living cells in a visible manner.



## 1. Introduction

Quantum dots (QDs) have become more attractive than traditional organic dyes for their promising properties, such as higher luminescence efficiency, excellent photostability, broad absorption and narrow emission spectra [1–3]. Therefore, as a new class of fluorescence probes, QDs have been extensively applied in fluorescence resonance energy transfer (FRET) assays [4–7], cellular structure labeling and in vivo long-term fluorescence imaging [8–16].

With the development of nanotechnology, many nanoscopic materials, such as nanoparticles [17–19], polymeric micelles [20], mesoporous silica nanorods [21] and nanotubes [22], etc. are now used as delivery vehicles. Drug encapsulation, cellular internalization and release are three challenges in the drug delivery systems [23]. In the context of release, several methods have been developed, such as hydrolysis under low pH [24], enzymatic degradation [25] and certain chemical reactions [26], etc. However, they are unable to be used directly in vivo. Recently, glutathione-triggered release systems have been used by Rotello's group for tunable reactivation of nanoparticle-inhibited beta-galactosidase [27], recovery of the transcriptional activity of nanoparticle-bound DNA [23], and release of dye molecules from monolayer protected nanoparticle carriers [28]. This trigger mechanism has attracted growing attention for two unique properties of GSH. First, GSH is ubiquitous in living systems and GSH/GSSG (glutathione disulfide) ratio provides an indicator for the redox environment of cells [29]. Second, intracellular concentration of GSH (e.g. 2 mM in erythrocytes [30], 10 mM in liver cells [31]) is significantly higher than that in the extracellular environment (e.g. 2 μM in red plasma [32]). This distinct concentration gradient of GSH provides a potential of GSH-dependent selective intracellular release. In addition, GSH is also selected as a stabilizer in synthesizing higher photoluminescence quantum yield (PL QY) and lower toxicity QDs, which are highly biocompatible and stable under physiological conditions [33,34].

In this paper, we reported that water-soluble and cysteamine protected CdTe QDs, which were positively charged in neutral condition, conjugated with plasmid DNA and formed larger complexes through simple electrostatic interaction. The formation of the QDs–DNA complexes almost completely inhibited the transcriptional activity of DNA. After being treated with GSH at intracellular concentrations, the entrapped DNA was released and recovered the ability to express the reporter protein in HEK 293 cells. The strong association and burst release mediated by GSH at intracellular concentrations without obviously injuring the

* Corresponding author. Tel.: +86 431 85262003; fax: +86 431 85689711.
** Corresponding author. Fax: +1 631 632 7960.
*E-mail addresses:* ekwang@ciac.jl.cn (E. Wang), jin.wang.1@stonybrook.edu (J. Wang).
[1] Dan Li and Gaiping Li contributed equally to this work.

0142-9612/$ – see front matter © 2008 Elsevier Ltd. All rights reserved.
doi:10.1016/j.biomaterials.2008.03.007

transcriptional viability of DNA implied that this positively charged QDs had the potential to be used as a new visible vehicle for gene or drug delivery in the future.

## 2. Materials and methods

### 2.1. Materials

Dulbecco's modified Eagle's medium (DMEM) was obtained from HyClone Corp. (USA). Trypsin was obtained from Amresco (USA). Fetal bovine serum (FBS) was obtained from Gibco (USA). GeneFinder™ was purchased from Bio-v Company (China). Lipotap reagent was obtained from Beyotime Company (Jiangsu, China). $NaBH_4$ (98%) was obtained from Acros. Plasmid DNA, pEGFP-C1 (4.9 kb, Clontech, Mountain View, CA, USA) was kept in DH5α. Midipreps DNA Purification System was obtained from Promega Corp., USA. HEK 293 cells (human embryonic kidney cell line) were obtained from Kunming Institute of Zoology, Chinese Academy of Sciences. All of the commercial products were used without further purification. Deionized water was purified by Milli-Q Purification System (Millipore).

### 2.2. Synthesis of 2-(dimethylamino) ethanethiol-capped CdTe QDs

The CdTe QDs were prepared in aqueous phase according to a one-pot method with a small modification [35]. Briefly, cadmium chloride ($CdCl_2$, 0.04 mol/L, 4 mL) was diluted to 50 mL in a one-neck flask. Then, trisodium citrate dihydrate (200 mg), $Na_2TeO_3$ (0.01 M, 1 mL), 2-(dimethylamino) ethanethiol hydrochloride (100 mg) and sodium borohydride ($NaBH_4$, 100 mg) were added with stirring. The pH value of the reaction system was adjusted by 1 M HCl to 5–6 [36]. The flask was attached to a condenser and refluxed at 100 °C under open-air conditions. The reaction was stopped when the fluorescence peak of as-prepared QDs was found to be located in red waveband region.

Absorption and fluorescence spectra of QDs samples were recorded at room temperature on a CARY 500 UV/vis-near-IR spectrophotometer (Varian) and a Perkin–Elmer LS-55 luminescence spectrometer, respectively.

### 2.3. Dye displacement assay

The processes of the QDs and DNA combination and dissociation were measured first by the dye displacement assay. This assay was modified from a reported procedure [37]. A quartz cuvette was loaded with Tris buffer (10 mM Tris–HCl, 10 mM NaCl, pH 7.4) and GeneFinder™ (final concentration, 0.125×). The plasmid DNA (pEGFP-C1, 10 μL, 0.02 μg/μL) was added and incubated for 5 min before reading the fluorescence intensity on a Perkin–Elmer LS-55 luminescence spectrometer (ex. 490 nm, em. 528 nm). Then, QDs solution was continuously added until the fluorescence intensity remained constant. This point was considered as the proper quantity of QDs to 200 ng DNA. This assay was also used to measure the release of DNA by GSH. GSH stock solution was added with certain final concentration (1 μM, 10 μM, 1 mM, 2 mM, 3 mM) and incubated at room temperature for 1 h. The fluorescence of the system was reported as relative intensity.

### 2.4. Electrophoretic mobility shift assay (EMSA)

EMSA samples were prepared by mixing QDs with pEGFP-C1 DNA (0.01 μg/μL) at different ratios according to the dye displacement assay. For the release assay, the solutions of QDs and DNA at stoichiometry were pre-incubated with different concentrations of GSH (10 μM, 1 mM, 3 mM) for gel electrophoresis. EMSA was performed by loading the above treated samples into 1.0 wt% agarose gel and ran at 100 V for approximately 40 min. Afterwards, the gel was incubated in 1 × GeneFinder™ solution for 4 h. Then the gel was photographed under UV light using a Vilber Lourmat Fluorescent Gel Imaging and Analysis System.

### 2.5. Zeta potential assay

Zeta potentials were measured by a MALVERN Zetasizer Nano ZS after QDs were pre-incubated without and with 1 mM of GSH in Tris buffer for 1 h. Three rounds of assays had been operated and the average data were analyzed and reported.

### 2.6. TEM characterization

The as-prepared aqueous suspension of QDs and the mixture of QDs and DNA were dropped onto carbon-coated copper grids separately and then dried under ambient conditions. The TEM images were obtained from a Hitachi H-8100 transmission electron microscope operating at an accelerating voltage of 200 kV.

### 2.7. XPS measurement

The deposit of QDs with DNA was dispersed in pure water or water containing 1 mM GSH, respectively. The latter sample was centrifuged after being incubated at room temperature for 1 h and redispersed in water. A drop of QDs as well as the above two as-prepared solutions was placed onto three clean silicon wafers separately and dried in air. X-ray photoelectron spectroscopy (XPS) measurements were performed on an ESCLABMKII spectrometer (VG Co., UK) using Al Kα radiation as the exciting source.

### 2.8. Cell culture and transfection experiment

HEK 293 cells were cultured in DMEM, supplemented with 10% fetal bovine serum (FBS) at 37 °C in a humidified 5% $CO_2$ incubator. The cells were seeded to a 96-well plate and incubated overnight. The wells were 60–80% confluent on the day of transfection. Lipotap mediated transfection was performed according to the manufacturer's instructions (Beyotime Company, China). After transfection, the cells were allowed to grow for another 48 h in the incubator. At that time, culture wells were usually 100% confluent. The fluorescence images were taken using a confocal laser scanning fluorescence microscope (CLSM, Leica TCS SP2). A flow cytometry (FCM, BD Biosciences) with an excitation wavelength of 488 nm was used to quantify the transfection efficiency of each sample. In this assay, the cells were detached from the culture plates by trypsin–EDTA (0.25% trypsin, 0.53 mM EDTA), washed with PBS for two times. The fluorescence intensity of EGFP was analyzed by the flow cytometry software.

## 3. Results and discussions

### 3.1. Dye displacement and zeta potential assays

Dye displacement assay is a simple, nondestructive, and high-throughput method for establishing DNA binding affinity, and ethidium bromide (EtBr) is a commonly used reagent for the assay [38]. We chose another dye, GeneFinder™ with similar function and lower toxicity, in place of EtBr to investigate the binding process of DNA to QDs as well as the release of DNA from the QDs–DNA complexes by GSH (Fig. 1). Point "a" presented the fluorescence of Tris buffer (the background). The diluted GeneFinder™ in the Tris buffer only gave a very weak fluorescence (point b). After the addition of 200 ng of pEGFP-C1 to the above solution, the fluorescence intensity of the system increased to point "c". The subsequent addition of QDs might convert the super-coiled plasmid DNA molecules into condensed ones [39] and extrude the inserted GeneFinder™, resulting in the decrease of the fluorescence intensity (c to d) [40]. At point "d", the GeneFinder™ was almost entirely quenched which demonstrated the complete conjugation of DNA molecules and QDs. Then, GSH was added to the system, when the final concentration reached 10 μM (the maximal concentration in extracellular environment [31,41]) only 15% of the total fluorescence intensity was recovered. With increasing the GSH concentration to 1 mM, the fluorescence intensity had reached to

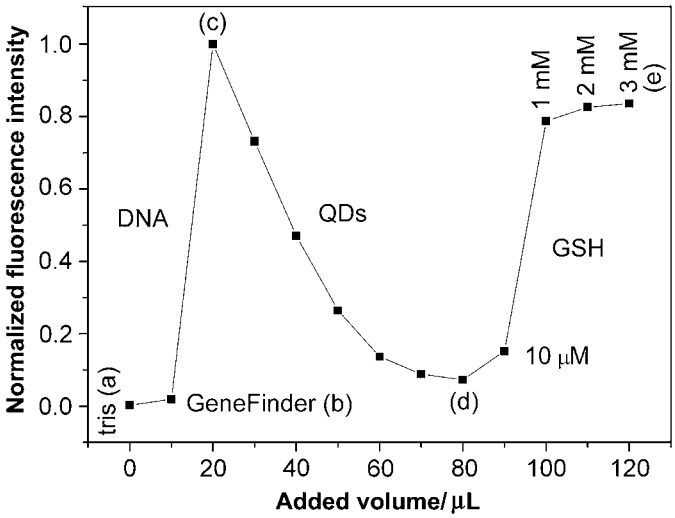


**Fig. 1.** The dye displacement assay: relative fluorescence intensity of GeneFinder™ was measured by successive adding (a to b) GeneFinder™, (b to c) plasmid DNA, (c to d) QDs, and (d to e) GSH. The fluorescence intensity of GeneFinder™–DNA mixture was defined as 1.0.

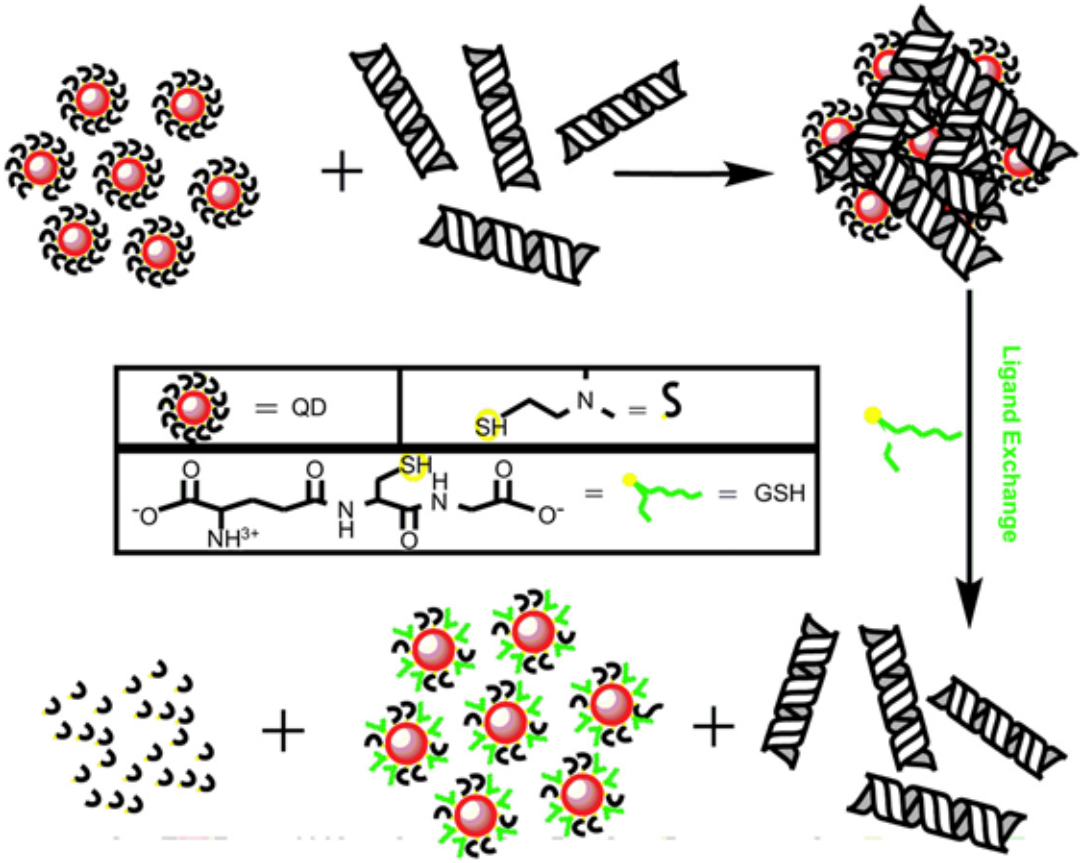


**Scheme 1.** Schematic illustration of QDs–DNA complexes structure and the process of GSH-mediated DNA release from the complexes.

79%. Further addition of GSH with the final concentrations to be 2 mM, 3 mM only resulted in slight fluorescence intensity increases to 82%, 83%, respectively. The release assay indicated that the 1 mM GSH was almost sufficient for disruption of the QDs–DNA complexes in our experiment.

The dye displacement assay demonstrated that GSH had the ability to release DNA from the QDs–DNA complexes in a concentration-dependent manner. In principle, negatively charged GSH containing a thiol ligand had stronger affinity to CdTe core. So we believed that the addition of GSH might counteract the positive charge of QDs to some extent by place exchange and resulted in dissociation of the QDs–DNA complexes (Scheme 1). The zeta potential measurement validated our above hypothesis. In this assay, upon the addition of 1 mM GSH, the zeta potential of QDs decreased significantly from $+26 \pm 4$ mV to $-12 \pm 2$ mV. It indicated that place exchange of the anionic GSH with the primary capping agent of the QDs diminished the overall positive charge of the QDs surface. This charge decrease would then be expected to reduce the affinity of QDs to DNA in our experiment.

### 3.2. Electrophoretic mobility shift assay (EMSA)

EMSA was used to confirm the complexation and dissociation reactions between QDs and DNA (Fig. 2). QDs completely inhibited the DNA from moving towards the positive electrode when the QDs/DNA was just at (lane C, 1/1) or excessive (lane D, 1.5/1) stoichiometry. It might be owing to the negative charges of DNA were counteracted by the positively charged QDs or the newly formed complexes were too large to enter the gel [42]. As expected, a small amount of DNA molecules were detected at the same site of pure plasmid DNA (lane A) when the QDs were not enough (lane B, QDs/DNA was 1/2). The mobility of DNA recovered completely when the final concentration of GSH reached 1 mM (lane F) and 3 mM (lane G), while there was no detectable DNA release when the QDs–DNA complexes were pre-treated with 10 μM GSH (lane E). The EMSA experiment was consistent with the result of dye displacement assay and displayed the complexation and dissociation processes in an intuitive way.

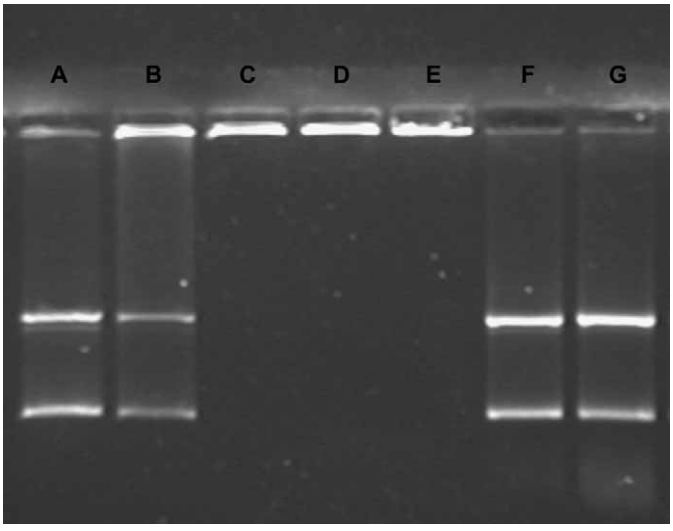


**Fig. 2.** The agarose gel electrophoresis of QDs and DNA mixture with different ratios (QDs/DNA in lanes A–D was 0/1, 1/2, 1/1 and 1.5/1 separately); the mixture of QDs and DNA at stoichiometry (1/1) incubated with different concentrations of GSH (lanes E–G: 10 μM, 1 mM, 3 mM). Each lane loaded with equal amount of DNA.

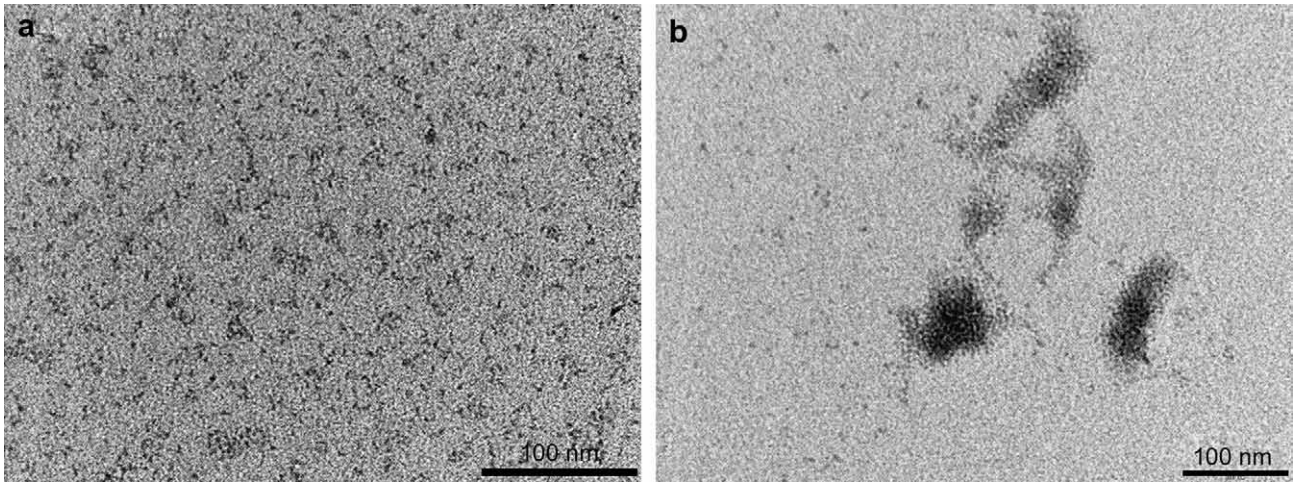


**Fig. 3.** TEM images of QDs (a) and QDs–DNA complexes (b).

### 3.3. TEM and XPS characterization

To further visualize the complexes formed by QDs and DNA, we took the TEM images of QDs alone and the QDs–DNA complexes (Fig. 3). The TEM images showed that CdTe QDs were monodisperse spherical particles with a mean diameter of 3.3 nm (a). After mixing with DNA, there were larger complexes appeared ranged from tens to several hundreds nanometers along with a few individual QDs (b).

XPS experiment was another accessorial evidence for the complexation and dissociation processes. As shown in Fig. 4, there was a P 2p peak (133.5 eV) in QDs–DNA complexes (b) which did not exist in the as-prepared QDs (a). This result demonstrated the presence of DNA in sample b. The decrease of the P 2p content in the QDs–DNA complexes after being treated with 1 mM GSH (c) indicated the reduction of DNA in the sample. It further confirmed that GSH could release DNA from the QDs–DNA complexes.

### 3.4. Transcriptional activity measurement of the released DNA

To testify whether the released plasmid DNA retained its transcriptional activity or not, we performed gene expression assay in HEK 293 cells with the assistance of Lipotap, a commercially available lipid-based transfection reagent. Fig. 5 showed the overlay images of the fluorescence and bright field pictures acquired from CLSM. There were only numberable green spots could be seen in the QDs–DNA complexes transfection sample (Fig. 5a). It indicated that the QDs–DNA complexes were stable and the transcriptional activity of the bound DNA was inhibited greatly by the QDs. When the QDs–DNA complexes were pre-incubated with 10 μM GSH, there was no obvious increase of cells expressed EGFP (Fig. 5b). However, there was a high level of EGFP expression with the QDs–DNA complexes pre-incubated by 1 mM GSH as shown in Fig. 5c, which was comparable with positive control that transfected equal quantity of pure DNA (Fig. 5f). It indicated that most of the released plasmid DNA retaining high transcriptional activity. It also should be noted that even though we added the QDs–DNA complexes with Lipotap to the cell culture and then GSH with a final concentration to be 1 mM, we also could see high level of EGFP expression (Fig. 5d). It indicated that the substance in the cell culture did not significantly affect GSH-mediated DNA release process in this experiment.

To further testify QDs did inhibit the DNA transcription, we firstly mixed the QDs with Lipotap thoroughly before adding plasmid DNA. After the transfection experiment, only fewer green spots could be seen in Fig. 5e compared with the positive control. It might be due to QDs competed with Lipotap for binding to DNA, and DNA bound by QDs could not be transcripted completely or at least to a large extent [23].

To quantify the transcriptional activity of released DNA, we measured the transfection efficiency by flow cytometry (FCM). In Fig. 6, we set the EGFP expression level of positive control as 100% (f). The FCM results of other samples corresponding to Fig. 5 were about 10% (a), 11% (b), 80% (c), 77% (d) and 34% (e), respectively. The

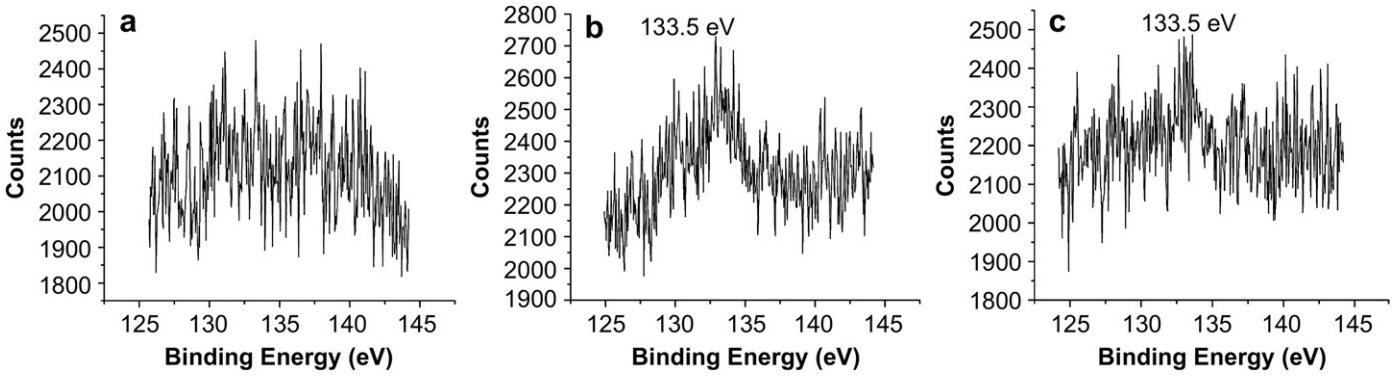


**Fig. 4.** XPS spectra characterized the content of P 2p (peak at 133.5 eV) in as-prepared QDs (a), QDs–DNA complexes (b), and QDs–DNA complexes after DNA released by 1 mM GSH (c).

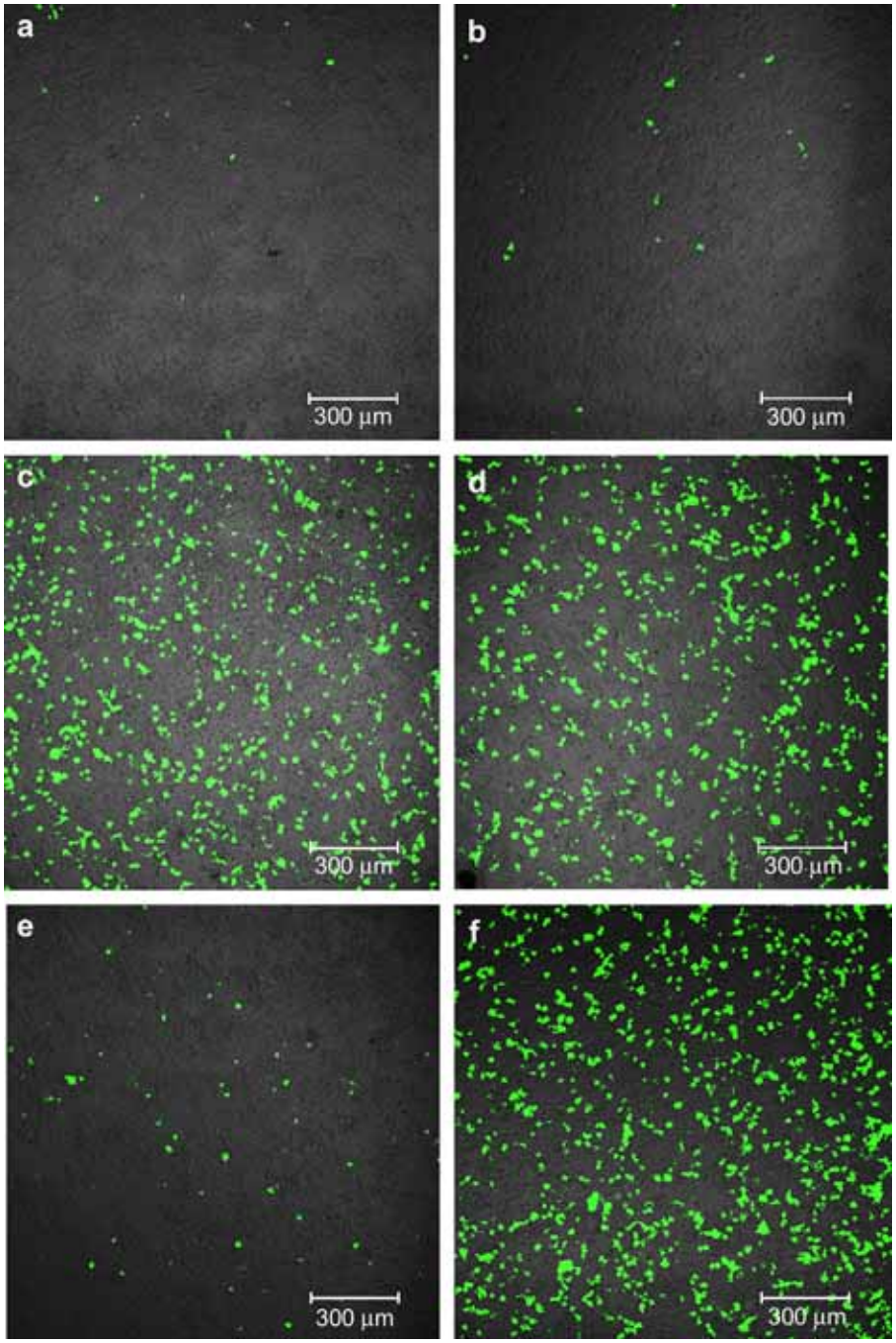


**Fig. 5.** The selected overlay CLSM images of EGFP fluorescence and bright field of HEK 293 cells were shown with 300 μm scale bars. The samples were transfected with QDs–DNA complexes (a); QDs–DNA complexes pre-incubated with 10 μM GSH (b); QDs–DNA complexes pre-incubated with 1 mM GSH (c); QDs–DNA complexes, then GSH was added to the cell culture with a final concentration of 1 mM (d); QDs and Lipotap were mixed firstly before DNA was added, then the mixture was used for transfection (e); and pure DNA (f). The pictures were obtained by a 10× objective.

CLSM and FCM statistic results of transfection experiment in HEK 293 cells proved that the DNA could be released by GSH at intracellular concentrations without distinctly injuring its transcriptional activity.

## 4. Conclusion

In summary, DNA could conjugate with the positively charged QDs through complementary electrostatic interaction to form the QDs–DNA complexes, which were disrupted by GSH at intracellular concentrations. Place exchange of the anionic GSH with the primary capping agent of the QDs diminished the overall positive charge of the QDs surface. We believed this was the reason of the controlled release. In addition, we demonstrated that the plasmid DNA released from the QDs–DNA complexes retained high transcriptional activity and expressed the reporter protein after being transfected into HEK 293 cells. The obvious gradient of GSH concentration in nature between the intra- and extracellular environments as well as the concentration-dependent triggered release without functional damage of the plasmid DNA implies the potential applications of the positively charged QDs in selective unpacking of payload in living cells with a visible manner in the future research.

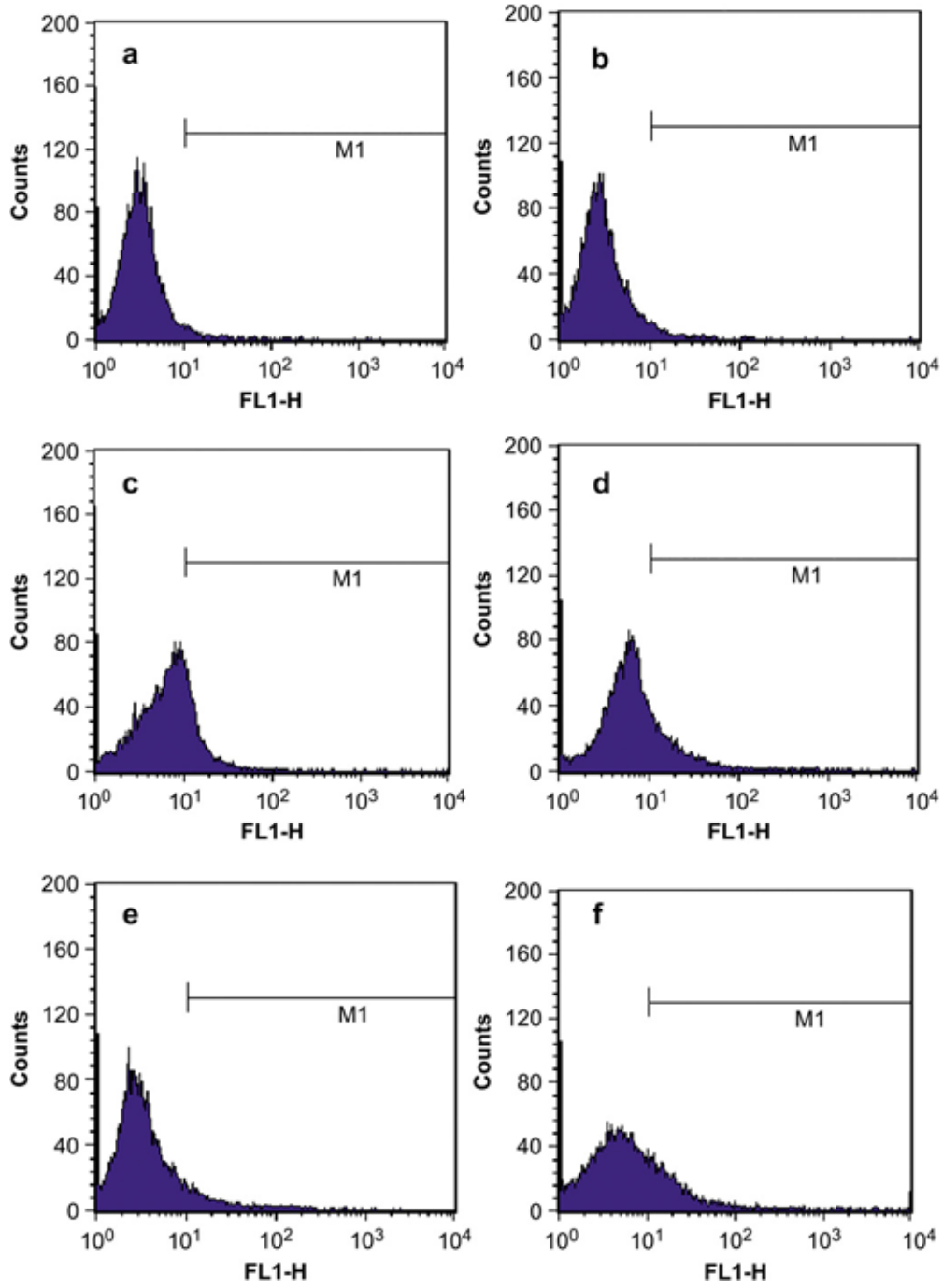


**Fig. 6.** Flow cytometry quantified the transfection efficiency in HEK 293 cells. It was a representative result of three separate experiments. The *x*-axis indicated the fluorescence intensity of EGFP. Images a–f presented the samples consistent with those in Fig. 5.

## Acknowledgements

This work was supported by National Natural Science Foundation of China (20575063, 20735003 and 90713022) and the Chinese Academy of Science KJCX2-YW-H09.

## References

[1] Alivisatos AP. Semiconductor clusters, nanocrystals, and quantum dots. Science 1996;271:933–7.
[2] Ho YP, Kung MC, Yang S, Wang TH. Multiplexed hybridization detection with multicolor colocalization of quantum dot nanoprobes. Nano Lett 2005;5:1693–7.
[3] Michalet X, Pinaud FF, Bentolila LA, Tsay JM, Doose S, Li JJ, et al. Quantum dots for live cells, in vivo imaging, and diagnostics. Science 2005;5709:538–44.
[4] Clapp AR, Medintz IL, Mauro JM, Fisher BR, Bawendi MG, Mattoussi H. Fluorescence resonance energy transfer between quantum dot donors and dye-labeled protein acceptors. J Am Chem Soc 2004;126:301–10.
[5] Clapp AR, Medintz IL, Uyeda HT, Fisher BR, Goldman ER, Bawendi MG, et al. Quantum dot-based multiplexed fluorescence resonance energy transfer. J Am Chem Soc 2005;127:18212–21.
[6] Ho YP, Chen HH, Leong KW, Wang TH. Evaluating the intracellular stability and unpacking of DNA nanocomplexes by quantum dots-FRET. J Control Release 2006;116:83–9.
[7] Shi L, DePaoli V, Rosenzweig N, Rosenzweig Z. Synthesis and application of quantum dots FRET-based protease sensors. J Am Chem Soc 2006;128:10378–9.
[8] Bruchez MJ, Moronne M, Gin P, Weiss S, Alivisatos AP. Semiconductor nanocrystals as fluorescent biological labels. Science 1998;281:2013–6.

[9] Chan WCW, Nie S. Quantum dot bioconjugates for ultrasensitive nonisotopic detection. Science 1998;281:2016–8.
[10] Parak WJ, Boudreau R, Gros ML, Gerion D, Zanchet D, Micheel CM, et al. Cell motility and metastatic potential studies based on quantum dot imaging of phagokinetic tracks. Adv Mater 2002;14:882–5.
[11] Jaiswal JK, Mattoussi H, Mauro JM, Simon SM. Long-term multiple color imaging of live cells using quantum dot bioconjugates. Nat Biotechnol 2003; 21:47–51.
[12] Dahan M, Levi S, Luccardini C, Rostaing P, Riveau B, Triller A. Diffusion dynamics of glycine receptors revealed by single-quantum dot tracking. Science 2003;302:442–5.
[13] Hanaki K-I, Momo A, Oku T, Komoto A, Maenosono S, Yamaguchi Y, et al. Semiconductor quantum dot/albumin complex is a long-life and highly photostable endosome marker. Biochem Biophys Res Commun 2003;302: 496–501.
[14] Wu X, Liu H, Liu J, Haley KN, Treadway JA, Larson JP, et al. Immunofluorescent labeling of cancer marker Her2 and other cellular targets with semiconductor quantum dots. Nat Biotechnol 2003;21:41–6.
[15] Sandros MG, Gao D, Benson DE. A modular nanoparticle-based system for reagentless small molecule biosensing. J Am Chem Soc 2005;127: 12198–9.
[16] Kaul Z, Yaguchi T, Harada JI, Ikeda Y, Hirano T, Chiura HX, et al. An antibody-conjugated internalizing quantum dot suitable for long-term live imaging of cells. Biochem Cell Biol 2007;85:133–40.
[17] Joshi HM, Bhumkar DR, Joshi K, Pokharkar V, Sastry M. Gold nanoparticles as carriers for efficient transmucosal insulin delivery. Langmuir 2006;22(1): 300–5.
[18] Paciotti GF, Myer L, Weinreich D, Goia D, Pavel N, McLaughlin RE, et al. Colloidal gold: a novel nanoparticle vector for tumor directed drug delivery. Drug Deliv 2004;11:169–83.
[19] Han G, Ghosh P, Rotello VM. Functionalized gold nanoparticles for drug delivery. Nanomedicine 2007;2:113–23.
[20] Savic R, Luo L, Eisenberg A, Maysinger D. Micellar nanocontainers distribute to defined cytoplasmic organelles. Science 2003;300:615–8.
[21] Giri S, Trewyn BG, Stellmaker MP, Lin VSY. Stimuli-responsive controlled-release delivery system based on mesoporous silica nanorods capped with magnetic nanoparticles. Angew Chem Int Ed Engl 2005;44: 5038–44.
[22] Son SJ, Reichel J, He B, Schuchman M, Lee SB. Magnetic nanotubes for magnetic-field-assisted bioseparation, biointeraction, and drug delivery. J Am Chem Soc 2005;127:7316–7.
[23] Han G, Chari NS, Verma A, Hong R, Martin CT, Rotello VM. Controlled recovery of the transcription of nanoparticle-bound DNA by intracellular concentrations of glutathione. Bioconjug Chem 2005;16: 1356–9.
[24] Ulbrich K, Subr V. Polymeric anticancer drugs with pH-controlled activation. Adv Drug Deliv Rev 2004;56:1023–50.
[25] Rooseboom M, Commandeur JNM, Vermeulen NPE. Enzyme-catalyzed activation of anticancer prodrugs. Pharmacol Rev 2004;56(1):53–102.
[26] Kam NWS, Liu Z, Dai H. Functionalization of carbon nanotubes via cleavable disulfide bonds for efficient intracellular delivery of siRNA and potent gene silencing. J Am Chem Soc 2005;127:12492–3.
[27] Verma A, Simard JM, Worrall JWE, Rotello VM. Tunable reactivation of nanoparticle-inhibited beta-galactosidase by glutathione at intracellular concentrations. J Am Chem Soc 2004;126:13987–91.
[28] Hong R, Han G, Fernandez JM, Kim BJ, Forbes NS, Rotello VM. Glutathione-mediated delivery and release using monolayer protected nanoparticle carriers. J Am Chem Soc 2006;128:1078–9.
[29] Wang QL, Wang SR, Ding Y, Peng KJ, Lin X, Qiao XR, et al. Age-related changes of the redox state of glutathione in plasma. Chin Med J 2005;118:1560–3.
[30] Hassan SSM, Rechnitz GA. Determination of glutathione and glutathione reductase with a silver sulfide membrane electrode. Anal Chem 1982;54: 1972–6.
[31] Anderson ME. Glutathione: an overview of biosynthesis and modulation. Chem Biol Interact 1998;112:1–14.
[32] Deberdt S, Castet S, Dandurand JL, Harrichoury JC, Louiset I, Jones DP, et al. Glutathione measurement in human plasma – evaluation of sample collection, storage and derivatization conditions for analysis of dansyl derivatives by HPLC. Clin Chim Acta 1998;275:175–84.
[33] Zheng YG, Gao SJ, Ying JY. Synthesis and cell-imaging applications of glutathione-capped CdTe quantum dots. Adv Mater 2007;19:376–80.
[34] Qian HF, Dong CQ, Weng JF, Ren JC. Facile one-pot synthesis of luminescent, water-soluble, and biocompatible glutathione-coated CdTe nanocrystals. Small 2006;2:747–51.
[35] Bao HF, Wang EK, Dong SJ. One-pot synthesis of CdTe nanocrystals and shape control of luminescent CdTe-cystine nanocomposites. Small 2006;2:476–80.
[36] Gaponik N, Talapin DV, Rogach AL, Hoppe K, Shevchenko EV, Kornowski A, et al. Thiol-capping of CdTe nanocrystals: an alternative to organometallic synthetic routes. J Phys Chem B 2002;106:7177–85.
[37] Boger DL, Fink BE, Brunette SR, Tse WC, Hedrick MP. A simple, high-resolution method for establishing DNA binding affinity and sequence selectivity. J Am Chem Soc 2001;123:5878–91.
[38] Kwon DS, Lin CH, Chen S, Coward JK, Walsh CT, Bollinger JM. Dissection of glutathionylspermidine synthetase/amidase from *Escherichia coli* into autonomously folding and functional synthetase and amidase domains. J Biol Chem 1997;272:2429–36.
[39] McIntosh CM, Esposito EA, Boal AK, Simard JM, Martin CT, Rotello VM. Inhibition of DNA transcription using cationic mixed monolayer protected gold clusters. J Am Chem Soc 2001;123:7626–9.
[40] Gershon H, Ghirlando R, Guttman SB, Minsky A. Mode of formation and structural features of DNA–cationic liposome complexes used for transfection. Biochemistry 1993;32:7143–51.
[41] Kobos RK, Parks SJ, Meyerhoff ME. Selectivity characteristics of potentiometric carbon dioxide sensors with various gas membrane materials. Anal Chem 1982;54:1976–80.
[42] Lynn DM, Langer R. Degradable poly(β-amino esters): synthesis, characterization, and self-assembly with plasmid DNA. J Am Chem Soc 2000;122: 10761–8.